Change detection between multi-band images using a robust fusion-based approach

Vinicius Ferraris, Nicolas Dobigeon, Qi Wei, Marie Chabert

CHANGE DETECTION BETWEEN MULTI-BAND IMAGES USING A ROBUST FUSION-BASED APPROACH

Vinicius Ferraris[(1)], *Nicolas Dobigeon*[(1)], *Qi Wei*[(2)] *and Marie Chabert*[(1)]

[(1)] University of Toulouse, IRIT/INP-ENSEEIHT, Toulouse, France
[(2)] University of Cambridge, Department of Engineering, UK
firstname.lastname@enseeiht.fr, qw245@cam.ac.uk

ABSTRACT

This paper proposes a robust fusion-based strategy to detect changes between two multi-band optical images with different spatial and spectral resolutions, e.g., a multispectral high spatial resolution image and a hyperspectral low spatial resolution image. The dissimilarity between sensor resolutions makes the change detection problem challenging, which has been generally bypassed in the literature: most often, the two images are crudely and independently resampled in order to get the same spatial and spectral resolutions and finally, classical change detection methods are applied. However, the resampling operation tends to lose information. In this paper, we propose a method that more effectively uses the available information: the two observed images are respectively modeled as spatial and spectral degradations of two latent images characterized by the same high spatial and high spectral resolutions. Representing the same scene, these latent images are expected to be globally similar except for possible changes in sparse spatial locations. Change detection is then envisioned through the solution of an inverse problem, shown to be a specific instance of multi-band image fusion. The proposed method is applied to real images with simulated realistic changes. A comparison with state-of-the-art change detection methods evidences the proposed method superiority.

Index Terms— change detection, hyperspectral, multispectral, resolution, optical images, heterogeneous sensors.

1. INTRODUCTION

Change detection (CD) is one of the most important issues in remote sensing. From long term monitoring to disaster management, change detection has innumerable applications [1]. CD compares the information collected from two or more multi-date images of the same geographical spot [2]. The scenario involving two images acquired through the same kind of sensors is the most favorable [3, 4]. However, current remote sensing imagery exploits many different kinds of sensors that provide, under different conditions of use, complementary information about the observed scene. Moreover, in some emergency situations such as natural disasters, it is not feasible, within a reasonable timeframe, to acquire new images of the same modality as that of already available ones. The need for flexibility and robustness against the diversity of image modalities motivates the investigation for new CD strategies.

Part of this work has been supported by Coordenação de Aperfeiçoamento de Ensino Superior (CAPES), Brazil, and EU FP7 through the ERANETMED JC-WATER Program, MapInvPlnt Project ANR-15-NMED-0002-02.

Optical images represent the most common remote sensing image modality [3, 4]. Currently appointed as multi-band optical images, they can be categorized according to their spatial and spectral resolutions [2]. The modalities referred to as panchromatic (PAN), multispectral (MS) and hyperspectral (HS) constitute a spectral classification of multi-band optical images according to an increasing number of spectral bands (respectively one, a dozen and hundreds) and consequently a decreasing spectral resolution. Considering the spatial dimension, images are qualified as high resolution (HR) or low resolution (LR) according to the size of the smallest object their constitutive pixels can represent.

The most common CD technique for optical single band images is based on image differencing following the assumptions of an additive Gaussian sensor noise and of identical spatial and spectral resolutions [4]. CD methods have been adapted to address the problem of optical images with increasing number of spectral bands. For instance, spectral change vector [5] and transform analysis [6, 7] allow the change information through all bands to be exploited. The approach proposed in [6] permits to deal with images of different spectral resolutions but still requires identical spatial resolutions.

This paper proposes a CD method able to deal with images of both dissimilar spatial and spectral resolutions. Typically, the two observed multi-band optical images are respectively a HR-MS (or HR-PAN) image and a LR-HS image. Each observed image can be considered as a spatial or spectral degradation of an unknown HR-HS latent image, where the term *degradation* here refers to the operation leading to the resolution decrease. The two latent images are characterized by the same spectral and spatial (high) resolutions. As they represent the same geographical location, they are expected to be characterized by a high degree of similarity. More precisely, changes in the scene are supposed to affect only specific and sparse spatial locations. Since the latent images have the same resolutions, it is now possible to build a so-called change vector. CD is then expressed as an inverse problem related to image fusion and solved within a Bayesian framework which allows one of the latent images and the change vector to be jointly inferred. The other latent image can be finally estimated as well as the changes.

This paper is organized as follows. Section 2 formulates the CD problem as a robust fusion task. In Section 3, the proposed fusion-driven CD algorithm is described. Section 4 analyzes the proposed method performance through simulations. Conclusions are reported in Section 5.

2. PROBLEM FORMULATION

Consider that the two observed multi-band optical images have been acquired over the same geographical area at two different times t_i

and t_j. Let $\mathbf{Y}_{\mathrm{HR}}^{t_i} \in \mathbb{R}^{n_\lambda \times n}$ denote the HR-MS/PAN image and $\mathbf{Y}_{\mathrm{LR}}^{t_j} \in \mathbb{R}^{m_\lambda \times m}$ the LR-HS image where m_λ (resp., n_λ) and m (resp. n) denote the numbers of bands and pixels of the HR-MS/PAN (resp. LR-HS) images with $m_\lambda > n_\lambda$ and $n > m$. Assuming that the scene has changed between their respective acquisition times, our objective is to extract the change information contained in this pair of dissimilar images. Due to the dissimilarity between the corresponding sensors, the differences in spectral and spatial resolutions makes the task difficult. Indeed, first, each pixel of the LR image is related to multiple pixels of the HR image. Second, the lack of spectral information in the MS/PAN image may hide some changes with respect to the HS image. To alleviate this issue, we propose to tackle the CD problem using a fusion-driven approach extending [8]. More precisely, these two observed images can be viewed as degradations of two HR-HS latent images representing the scene at times t_i and t_j respectively. The joint observation model can be written as

$$\begin{aligned} \mathbf{Y}_{\mathrm{HR}}^{t_i} &= \mathbf{L}\mathbf{X}^{t_i} + \mathbf{N}_{\mathrm{HR}} \\ \mathbf{Y}_{\mathrm{LR}}^{t_j} &= \mathbf{X}^{t_j}\mathbf{R} + \mathbf{N}_{\mathrm{LR}} \end{aligned} \tag{1}$$

where $\mathbf{X}^{t_i}, \mathbf{X}^{t_j} \in \mathbb{R}^{m_\lambda \times n}$ represent the latent HS-HR images at time t_i and t_j. The matrix $\mathbf{L} \in \mathbb{R}^{n_\lambda \times m_\lambda}$ is the spectral degradation matrix modeling the linear combination of some spectral bands for each pixel and $\mathbf{R} = \mathbf{BS} \in \mathbb{R}^{n \times m}$ is the spatial degradation matrix modeling the linear combination of pixels within each spectral band. The two matrices $\mathbf{B}$ and $\mathbf{S}$ correspond to a band-wise spatially invariant blur and a band-wise spatial decimation operator, respectively, and can be estimated beforehand as in [9]. The additive noise matrices, $\mathbf{N}_{\mathrm{LR}}$ and $\mathbf{N}_{\mathrm{HR}}$, gather sensor noises and modeling errors. They are generally modeled as mutually independent (since they are associated to different sensors) and following matrix normal distributions [1] [10]

$$\begin{aligned} \mathbf{N}_{\mathrm{HR}} &\sim \mathcal{MN}_{n_\lambda, n}(\mathbf{0}_{n_\lambda \times n}, \mathbf{\Lambda}_{\mathrm{HR}}, \mathbf{I}_n) \\ \mathbf{N}_{\mathrm{LR}} &\sim \mathcal{MN}_{m_\lambda, m}(\mathbf{0}_{m_\lambda \times m}, \mathbf{\Lambda}_{\mathrm{LR}}, \mathbf{I}_m). \end{aligned} \tag{2}$$

where $\mathbf{\Lambda}_{\mathrm{HR}}$ and $\mathbf{\Lambda}_{\mathrm{LR}}$ denote the row-wise covariance matrices corresponding to spectral correlations between spectral bands of the HR and LR noises. The HR and LR column-wise covariance matrices are assumed to be identity matrices $\mathbf{I}_n$ and $\mathbf{I}_m$ to traduce the independence of the noise sensors with respect to pixel locations.

The use of the latent images $\mathbf{X}^{t_i}$ and $\mathbf{X}^{t_j}$ makes the CD problem simpler: indeed, they are pixel-wise comparable since they share the same spatial and spectral resolutions. Moreover, they are expected to have a certain degree of similarity since they represent the same geographical location. As the acquisition times can be switched, this hypothesis allows each latent image to be related to the other one through an additive change matrix $\mathbf{\Delta X}$

$$\mathbf{X}^{t_i} = \mathbf{X}^{t_j} + \mathbf{\Delta X}. \tag{3}$$

This term should account for significant changes in the observed scene and is expected to exhibit spatial sparsity. As a consequence, the CD problem can be formulated as the joint estimation of the latent image $\mathbf{X}^{t_j}$ and the change matrix $\mathbf{\Delta X}$, where the complementary image $\mathbf{X}^{t_i}$ can be obtained as a by-product using the additive model (3). It is worthy to note that, when $\mathbf{\Delta X} = \mathbf{0}$, this task comes down to the multi-band image fusion problem addressed in [11–13] and more recently in [14–19]. Following these works, we propose to solve this problem within a Bayesian framework by designing appropriate prior distributions (i.e., regularizations) for the unknown parameters $\mathbf{X}^{t_j}$ and $\mathbf{\Delta X}$ to be inferred. The resulting so-called *robust* multi-band image fusion approach is described in what follows.

3. ROBUST MULTI-BAND IMAGE FUSION

3.1. Objective function

The proposed robust fusion-driven CD approach consists of recovering the latent image $\mathbf{X}^{t_j}$ and the change matrix $\mathbf{\Delta X}$ given the forward model (1), the noise statistics assumed in (2) and the additional assumption (3) relating the two latent images. The additive and matrix normal model for each noise matrices in (2) leads to a matrix normal distribution for each observed $\mathbf{Y}_{\mathrm{HR}}^{t_i}$ and $\mathbf{Y}_{\mathrm{LR}}^{t_j}$:

$$\begin{aligned} \mathbf{Y}_{\mathrm{HR}}^{t_i} | \mathbf{X}^{t_i} &\sim \mathcal{MN}_{n_\lambda, n}(\mathbf{L}\mathbf{X}^{t_i}, \mathbf{\Lambda}_{\mathrm{HR}}, \mathbf{I}_n) \\ \mathbf{Y}_{\mathrm{LR}}^{t_j} | \mathbf{X}^{t_j} &\sim \mathcal{MN}_{m_\lambda, m}(\mathbf{X}^{t_j}\mathbf{BS}, \mathbf{\Lambda}_{\mathrm{LR}}, \mathbf{I}_m). \end{aligned} \tag{4}$$

Since the sensor and model noises are assumed statistically independent, the observed images can be assumed statistically independent as well. Thus, their joint likelihood function can be written as the product of the conditional distributions $p(\mathbf{Y}_{\mathrm{HR}}^{t_i} | \mathbf{X}^{t_i})$ and $p(\mathbf{Y}_{\mathrm{LR}}^{t_j} | \mathbf{X}^{t_j})$. The joint maximum a posteriori (MAP) estimator of the latent and change images, assumed to be a priori independent, can be expressed by minimizing the resulting negative log-posterior

$$\left\{ \hat{\mathbf{X}}_{\mathrm{MAP}}^{t_j}, \mathbf{\Delta}\hat{\mathbf{X}}_{\mathrm{MAP}} \right\} \in \underset{\mathbf{X}^{t_j}, \mathbf{\Delta X}}{\mathrm{Argmin}} \, \mathcal{J}(\mathbf{X}^{t_j}, \Delta\mathbf{X}) \tag{5}$$

with

$$\begin{aligned} \mathcal{J}(\mathbf{X}^{t_j}, \Delta\mathbf{X}) = & \left\| \mathbf{\Lambda}_{\mathrm{LR}}^{-\frac{1}{2}} \left(\mathbf{Y}_{\mathrm{LR}}^{t_j} - \mathbf{X}^{t_j}\mathbf{BS} \right) \right\|_F^2 \\ & + \left\| \mathbf{\Lambda}_{\mathrm{HR}}^{-\frac{1}{2}} \left(\mathbf{Y}_{\mathrm{HR}}^{t_i} - \mathbf{L}\left(\mathbf{X}^{t_j} + \Delta\mathbf{X} \right) \right) \right\|_F^2 \\ & + \lambda\phi_1\left(\mathbf{X}^{t_j} \right) + \gamma\phi_2\left(\Delta\mathbf{X} \right) \end{aligned} \tag{6}$$

where $\|\cdot\|_F$ stands for the Frobenius norm. The penalizing functions $\phi_1(\cdot)$ and $\phi_2(\cdot)$ can be related to the negative log-prior distributions of the latent and change images, respectively, and the parameters λ and γ tune the amount of corresponding regularizations in the overall objective function $\mathcal{J}(\mathbf{X}^{t_j}, \Delta\mathbf{X})$.

These functions should be carefully designed to exploit prior information regarding the parameter of interest. Problems similar to (5) have been considered in many applications involving optical multi-band images specially those related to image restoration. In the context of multi-band fusion, as mentioned earlier, $\Delta\mathbf{X} = 0$ and the purpose is to obtain a single HR-HS latent image fairly gathering the information contained in the observed ones. In this context, various penalizing functions $\phi_1(\cdot)$ have been considered in the literature, including Tikhonov, dictionary-based and total-variation [18, 19]. In this work, a Tikhonov regularization has been chosen to maintain computational efficiency while providing accurate results [20]. Conversely, in the context of CD, we propose to recover two different latent images and $\phi_2(\cdot)$ should reflect the fact that most of the pixels are expected to remain unchanged in $\mathbf{X}^{t_1}$ and $\mathbf{X}^{t_j}$, i.e., most of

[1] The probability density function, $p(\mathbf{X}|\mathbf{M}, \mathbf{\Sigma}_c, \mathbf{\Sigma}_r)$ of a matrix normal distribution $\mathcal{MN}_{r,c}(\mathbf{M}, \mathbf{\Sigma}_r, \mathbf{\Sigma}_c)$ is given by

$$p\left(\mathbf{X}|\mathbf{M}, \mathbf{\Sigma}_r, \mathbf{\Sigma}_r\right) = \frac{\exp\left(-\frac{1}{2} tr\left[\mathbf{\Sigma}_c^{-1} \left(\mathbf{X} - \mathbf{M} \right)^T \mathbf{\Sigma}_r^{-1} \left(\mathbf{X} - \mathbf{M} \right) \right] \right)}{(2\pi)^{rc/2} \left| \mathbf{\Sigma}_c \right|^{r/2} \left| \mathbf{\Sigma}_r \right|^{c/2}}$$

where $\mathbf{M} \in \mathbb{R}^{r \times c}$ is the mean matrix, $\mathbf{\Sigma}_r \in \mathbb{R}^{r \times r}$ is the row covariance matrix and $\mathbf{\Sigma}_c \in \mathbb{R}^{c \times c}$ is the column covariance matrix.

the columns of the change image $\mathbf{\Delta X}$ are expected to be null vectors. Consequently, the following $\ell_{2,1}$-norm regularization term is considered [21, 22]

$$\phi_2\left(\Delta\mathbf{X}\right) = \left\|\Delta\mathbf{X}\right\|_{2,1} = \sum_{p=1}^{n} \left\|\Delta\mathbf{x}_p\right\|_2 \tag{7}$$

with $\Delta\mathbf{X} = [\Delta\mathbf{x}_1, \ldots, \Delta\mathbf{x}_n]$.

3.2. Block coordinate algorithm

The objective function (6) is iteratively minimized following an iterative block coordinate descent (BCD) algorithm summarized in Algo. 1. It iteratively minimizes the objective function with respect to (w.r.t.) the individual variables $\mathbf{X}^{t_j}$ and $\Delta\mathbf{X}$ and thus allows the full problem to be split into two sub-problems. These sub-problems can be efficiently solved separately according to different strategies as detailed below.

Algorithm 1 BCD algorithm for robust multi-band image fusion

Input: $\mathbf{Y}_{\mathrm{LR}}^{t_j}, \mathbf{Y}_{\mathrm{HR}}^{t_i}, \mathbf{L}, \mathbf{B}, \mathbf{S}, \Delta\mathbf{X}_0$.
1: **for** $k = 1, 2, \cdots$ **to** stopping rule **do**
2: $\quad \mathbf{X}_k^{t_j} = \arg\min \mathcal{J}(\mathbf{X}^{t_j}, \Delta\mathbf{X}_{k-1})$
3: $\quad \Delta\mathbf{X}_k = \arg\min \mathcal{J}(\mathbf{X}_k^{t_j}, \Delta\mathbf{X})$
4: **end for**
Output: $\hat{\mathbf{X}}^{t_j}, \Delta\hat{\mathbf{X}}$

3.2.1. Minimization with respect to $\mathbf{X}^{t_j}$

By setting $\Delta\mathbf{X} = \Delta\mathbf{X}_k$ in (6), let us define the HR-MS pseudo-observed image at time t_j as

$$\widetilde{\mathbf{Y}}_{\mathrm{HR},k}^{t_j} = \mathbf{Y}_{\mathrm{HR}}^{t_i} - \mathbf{L}\Delta\mathbf{X}_k. \tag{8}$$

Note that this quantity does not correspond to any observation but rather stands for the potentially observed HR-MS image at time t_j according to the current value of the change vector $\Delta\mathbf{X}_k$. The introduction of (8) into (6) leads to the objective function w.r.t. $\mathbf{X}^{t_j}$

$$\begin{aligned}\mathcal{J}(\mathbf{X}^{t_j}, \Delta\mathbf{X}_{k-1}) = &\left\|\mathbf{\Lambda}_{\mathrm{LR}}^{-\frac{1}{2}}\left(\mathbf{Y}_{\mathrm{LR}}^{t_j} - \mathbf{X}^{t_j}\mathbf{BS}\right)\right\|_F^2 \\ &+ \left\|\mathbf{\Lambda}_{\mathrm{HR}}^{-\frac{1}{2}}\left(\widetilde{\mathbf{Y}}_{\mathrm{HR},k}^{t_j} - \mathbf{L}\mathbf{X}^{t_j}\right)\right\|_F^2 + \lambda\phi_1\left(\mathbf{X}^{t_j}\right).\end{aligned} \tag{9}$$

The sub-problem defined by (9) amounts to the image fusion problem considered in [16–18]. The objective is indeed to estimate a single latent image $\mathbf{X}^{t_j}$ from two observed images of the same scene. The only difference is that one of the observed images is replaced by a pseudo-observation. There exists a broad literature covering this problem. Recently, [18] proposed an explicit solution by setting the derivative w.r.t. the latent image to zero. The problem then reduces to a *Sylvester equation* that can be explicitly solved under particular conditions with a far lower computational complexity than other state-of-the-art methods (see [18] for more details).

3.2.2. Minimization with respect to $\Delta\mathbf{X}$

The same strategy can be followed for the second sub-problem. By fixing $\mathbf{X}^{t_j} = \mathbf{X}_k^{t_j}$ in (6), let us define the HR-MS change image by

$$\Delta\widetilde{\mathbf{Y}}_{\mathrm{HR},k} = \mathbf{Y}_{\mathrm{HR}}^{t_i} - \mathbf{L}\mathbf{X}_k^{t_j}. \tag{10}$$

As in section 3.2.1, this unobserved quantity stands for the change image between the HR-MS observed image and a pseudo-observed HR-MS image resulting from the current state $\mathbf{X}_k^{t_j}$ of the HR-HS latent image estimate. The introduction of (10) in (6) leads to the objective function w.r.t $\Delta\mathbf{X}$

$$\mathcal{J}(\mathbf{X}_k^{t_j}, \Delta\mathbf{X}) = \left\|\mathbf{\Lambda}_{\mathrm{HR}}^{-\frac{1}{2}}\left(\Delta\widetilde{\mathbf{Y}}_{\mathrm{HR},k} - \mathbf{L}\Delta\mathbf{X}\right)\right\|_F^2 + \gamma\phi_2\left(\Delta\mathbf{X}\right). \tag{11}$$

With the particular choice of $\phi_2(\cdot)$ conducted in Section 3.1, both data-fitting and regularization terms are convex [23], despite the latter one is not smooth. One way to achieve the unique solution is by means of proximal algorithms [24]. In particular, the forward-backward splitting algorithm [25] addressed problems with the same structure as the stated one. Consequently, it does not require additional considerations but the definition of the appropriate proximal operators and the first order derivatives (see [26] for more details).

4. EXPERIMENTAL RESULTS

This Section analyzes the performance of the proposed CD method. Real data for CD with associated ground truth (i.e., real binary CD mask) is rarely available. Thus, to test the proposed method, a simulation setup inspired by the Wald's protocol [27] has been used to generate the observed and latent images from a single reference HR-HS image. The reference image is a pre-corrected $610 \times 330 \times 93$ HS image of the Pavia University in Italy acquired by the ROSIS (reflective optics system imaging spectrometer) sensor. Two spectral degradations were considered: one corresponding to a 4-band LANDSAT multi-spectral response (Scenario 1) and a 43-band averaging panchromatic response (Scenario 2). The spatial degradation response consists in a 5×5 Gaussian blur with equal down-sampling by $d = 5$ in vertical and horizontal directions. The resulting HR-MS and LR-HS images are depicted in Fig. 1 (a)-(b) for Scenario 1. From a single HR-HS reference image, several change masks were manually generated. For each change mask a change has been applied, for instance, by replacing the whole change mask region by different pixels, or by rotating its content. The constructed simulation dataset is composed of 225 different HR-HS pairs. By applying the defined spatial and spectral responses in each image of the HR-HS pair alternately, two observation image pairs of LR-MS/PAN and HR-HS and their respective ground-truth change maps compose the whole simulation dataset. The proposed robust fusion-based change detection (RF) method is compared to three algorithms. They differ in the preprocessing used to handle images with the same resolution. In any case, CD is performed using the approach described in [7]. The first algorithm compares the spatially degraded version of the HR-MS image with the spectrally degraded version of the LR-HS image. The resulting LR change map is denoted as $\hat{\mathbf{D}}_{\mathrm{WC}}$ where WC means worst-case. The second algorithm performs a bi-cubic spatial interpolation of the LR-HS image, spectrally degrades the result and finally performs CD by comparison with the original HR-MS image. The resulting change map is denoted as $\hat{\mathbf{D}}_{\mathrm{ID}}$ where ID means interpolation-degradation. The third algorithm uses the same procedure of the second one except that the order of interpolation and degradation operations is changed. The resulting change detection map is denoted as $\hat{\mathbf{D}}_{\mathrm{DI}}$ where DI refers to degradation-interpolation.

The performance of CD methods is evaluated by investigating the receiving operator characteristics (ROC) curve, which plots the probability of false alarm (PFA) as a function of the probability of detection (PD). Each sample of the dataset results in one ROC

(a) (b) (c) (d) (e)

Fig. 1: Scenario 1: (a) $\mathbf{Y}_{\mathrm{HR}}^{t_i}$, (b) $\mathbf{Y}_{\mathrm{LR}}^{t_j}$, (c) $\hat{\mathbf{X}}^{t_i}$, (d) $\hat{\mathbf{X}}^{t_j}$ and (e) $\Delta\hat{\mathbf{X}}$

curve. The final result for each CD method is the averaging of all dataset ROC curves. Figure 2 presents the averaged ROC curves obtained with the four methods in two different scenarios corresponding to HR-MS/LR-HS (Scenario 1) and HR-PAN/LR-HS (Scenario 2) image pairs.

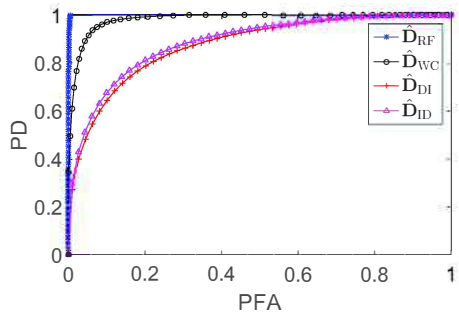

(a)

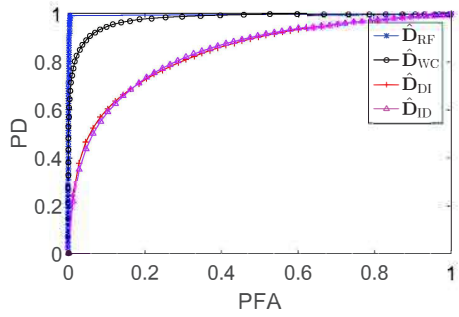

(b)

Fig. 2: Final ROC curves: (a) Scenario 1 and (b) Scenario 2.

Additionally, two quantitative measures of detection performance can be extracted from these ROC curves: the area under the curve (AUC), corresponding to the integration of the ROC curve and the distance (Dist.) between the interception of the ROC curve with the diagonal line, $\mathrm{PFA} = 1 - \mathrm{PD}$, and the no detection point $(\mathrm{PFA} = 1, \mathrm{PD} = 0)$. In both cases, the better the detection the closer to one the measure.

For both scenarios, the proposed method shows higher detection performance than the other methods. To illustrate the high precision and the benefits of the proposed algorithm, Fig. 1 represents one example of the results recovered by the proposed CD method in the Scenario 1. In this example, two HR-MS and LR-HS observed images have been fused producing the pair of latent images $\left(\hat{\mathbf{X}}^{t_i}, \hat{\mathbf{X}}^{t_i}\right)$ (panels (c) and (d)) and the change image $\Delta\hat{\mathbf{X}}$ (panel (e)). Note that complementary simulation results are available in [26].

Table 1: Detection performance (AUC and normalized distance).

		$\hat{\mathbf{D}}_{\mathrm{RF}}$	$\hat{\mathbf{D}}_{\mathrm{WC}}$	$\hat{\mathbf{D}}_{\mathrm{DI}}$	$\hat{\mathbf{D}}_{\mathrm{ID}}$
Scenario 1	AUC	**0.9974**	0.9809	0.8724	0.8850
	Dist.	**0.9944**	0.9356	0.7926	0.8045
Scenario 2	AUC	**0.9936**	0.9777	0.8389	0.8389
	Dist.	**0.9896**	0.9249	0.7595	0.7640

5. CONCLUSIONS

This paper proposed a new change detection method to deal with multi-band optical images with different spatial and spectral resolutions. Changes may be thought of as the differences between two unknown latent images of same (high) spatial and spectral resolutions. Based on the degradation model relating each observed image to its associated latent one, a Bayesian estimation method was adopted to infer the two latent images and the associated change vector. The estimation problem was formulated as an inverse problem and solved iteratively using a block coordinate descent algorithm. By fixing alternatively one of the two variables, the algorithm allowed the problem to be split into two distinct sub-problems, the estimation of one latent image and the estimation of the change vector. The first sub-problem was a classical image fusion problem benefiting from an explicit solution. The second sub-problem was regularized taking into account the spatial sparsity of significant changes. At the end, the second latent image can be estimated by subtracting the estimated latent image by the estimated change vector. The proposed method showed far higher detection performance than naive approaches which would enforce the data to be of the same low spatial and spectral resolution.

6. REFERENCES

[1] M. D. Mura, S. Prasad, F. Pacifici, P. Gamba, J. Chanussot, and J. A. Benediktsson, "Challenges and opportunities of multimodality and data fusion in remote sensing," *Proc. IEEE*, vol. 103, no. 9, pp. 1585–1601, Sept. 2015.

[2] J. B. Campbell and R. H. Wynne, *Introduction to remote sensing*, 5th ed. Guilford Press, 2011.

[3] R. J. Radke, S. Andra, O. Al-Kofahi, and B.Roysam, "Image change detection algorithms: a systematic survey," *IEEE Trans. Image Process.*, vol. 14, no. 3, pp. 294–307, 2005.

[4] F. Bovolo and L. Bruzzone, "The time variable in data fusion: A change detection perspective," *IEEE Geosci. Remote Sens. Mag.*, vol. 3, no. 3, pp. 8–26, Sept. 2015.

[5] ——, "A theoretical framework for unsupervised change detection based on change vector analysis in the polar domain," *IEEE Trans. Geosci. Remote Sens.*, vol. 45, no. 1, pp. 218–236, Jan. 2007.

[6] A. Nielsen, K. Conradsen, and J. Simpson, "Multivariate alteration detection (MAD) and MAF postprocessing in multispectral, bitemporal image data: New approaches to change detection studies," *Remote Sens. Environment*, vol. 64, no. 1, pp. 1–19, 1998.

[7] A. Nielsen, "The regularized iteratively reweighted MAD method for change detection in multi- and hyperspectral data," *IEEE Trans. Image Process.*, vol. 16, no. 2, pp. 463–478, Feb. 2007.

[8] V. Ferraris, N. Dobigeon, Q. Wei, and M. Chabert, "Detecting changes between optical images of different spatial and spectral resolutions: a fusion-based approach," 2017, submitted.

[9] N. Yokoya, N. Mayumi, and A. Iwasaki, "Cross-calibration for data fusion of EO-1/Hyperion and Terra/ASTER," *IEEE J. Sel. Topics Appl. Earth Observations Remote Sens.*, vol. 6, no. 2, pp. 419–426, April 2013.

[10] A. K. Gupta and D. K. Nagar, *Matrix Variate Distribution*, ser. Monographs and Surveys in Pure and Applied Mathematics. Chapman and Hall, 1999, no. 104.

[11] R. C. Hardie, M. T. Eismann, and G. L. Wilson, "MAP estimation for hyperspectral image resolution enhancement using an auxiliary sensor," *IEEE Trans. Image Process.*, vol. 13, no. 9, pp. 1174–1184, Sept. 2004.

[12] M. T. Eismann and R. C. Hardie, "Hyperspectral resolution enhancement using high-resolution multispectral imagery with arbitrary response functions," *IEEE Trans. Image Process.*, vol. 43, no. 3, pp. 455–465, March 2005.

[13] Y. Zhang, S. De Backer, and P. Scheunders, "Noise-resistant wavelet-based Bayesian fusion of multispectral and hyperspectral images," *IEEE Trans. Geosci. Remote Sens.*, vol. 47, no. 11, pp. 3834–3843, Nov. 2009.

[14] N. Yokoya, T. Yairi, and A. Iwasaki, "Coupled nonnegative matrix factorization unmixing for hyperspectral and multispectral data fusion," *IEEE Trans. Geosci. Remote Sens.*, vol. 50, no. 2, pp. 528–537, Feb. 2012.

[15] M. Simões, J. Bioucas Dias, L. Almeida, and J. Chanussot, "A convex formulation for hyperspectral image superresolution via subspace-based regularization," *IEEE Trans. Geosci. Remote Sens.*, vol. 6, no. 53, pp. 3373–3388, June 2015.

[16] Q. Wei, N. Dobigeon, and J.-Y. Tourneret, "Bayesian fusion of multi-band images," *IEEE J. Sel. Topics Signal Process.*, vol. 9, no. 6, pp. 1117–1127, Sept. 2015.

[17] Q. Wei, J. Bioucas-Dias, N. Dobigeon, and J.-Y. Tourneret, "Hyperspectral and multispectral image fusion based on a sparse representation," *IEEE Trans. Geosci. Remote Sens.*, vol. 53, no. 7, pp. 3658–3668, 2015.

[18] Q. Wei, N. Dobigeon, and J.-Y. Tourneret, "Fast fusion of multi-band images based on solving a Sylvester equation," *IEEE Trans. Image Process.*, vol. 24, no. 11, pp. 4109–4121, Nov. 2015.

[19] Q. Wei, N. Dobigeon, J.-Y. Tourneret, J. M. Bioucas-Dias, and S. Godsill, "R-FUSE: Robust fast fusion of multi-band images based on solving a Sylvester equation," *IEEE Signal Process. Lett.*, vol. 23, no. 11, pp. 1632–1636, Nov. 2016.

[20] L. Loncan, L. de Almeida, J. M. Bioucas-Dias, X. Briottet, J. Chanussot, N. Dobigeon, S. Fabre, W. Liao, G. A. Licciardi, M. Simoes, J.-Y. Tourneret, M. Veganzones, G. Vivone, Q. Wei, and N. Yokoya, "Hyperspectral pansharpening: A review," *IEEE Geosci. Remote Sens. Mag.*, vol. 3, no. 3, pp. 27–46, Sept. 2015.

[21] C. Févotte and N. Dobigeon, "Nonlinear hyperspectral unmixing with robust nonnegative matrix factorization," *IEEE Trans. Image Process.*, vol. 24, no. 12, pp. 4810–4819, 2015.

[22] S. J. Wright, R. D. Nowak, and M. A. T. Figueiredo, "Sparse reconstruction by separable approximation," *IEEE Trans. Signal Process.*, vol. 57, no. 7, pp. 2479–2493, July 2009.

[23] S. Boyd and L. Vandenberghe, *Convex optimization.* Cambridge University Press, 2004.

[24] N. Parikh and S. Boyd, "Proximal algorithms," *Foundations and Trends in Optimization*, vol. 1, no. 3, pp. 127–239, 2014.

[25] P. Combettes and J. Pesquet, "Proximal splitting methods in signal processing," *Fixed-Point Algorithm for Inverse Problems in Science and Engineering*, pp. 185–212, 2011.

[26] V. Ferraris, N. Dobigeon, Q. Wei, and M. Chabert, "Robust fusion of multi-band images with different spatial and spectral resolutions for change detection," 2017, submitted.

[27] L. Wald, T. Ranchin, and M. Mangolini, "Fusion of satellite images of different spatial resolutions: assessing the quality of resulting images," *Photogrammetric engineering and remote sensing*, vol. 63, no. 6, pp. 691–699, 1997.